Control of Kinetic Properties of AMPA Receptor Channels by Nuclear RNA Editing

Hilda Lomeli,* Johannes Mosbacher, Thorsten Melcher, Thomas Höger, Jörg R. P. Geiger, Thomas Kuner, Hannah Monyer, Miyoko Higuchi, Alfred Bach, Peter H. Seeburg†

AMPA (α-amino-3-hydroxy-5-methyl-4-isoxazolepropionic acid) receptor channels mediate the fast component of excitatory postsynaptic currents in the central nervous system. Site-selective nuclear RNA editing controls the calcium permeability of these channels, and RNA editing at a second site is shown here to affect the kinetic aspects of these channels in rat brain. In three of the four AMPA receptor subunits (GluR-B, -C, and -D), intronic elements determine a codon switch (AGA, arginine, to GGA, glycine) in the primary transcripts in a position termed the R/G site, which immediately precedes the alternatively spliced modules "flip" and "flop." The extent of editing at this site progresses with brain development in a manner specific for subunit and splice form, and edited channels possess faster recovery rates from desensitization.

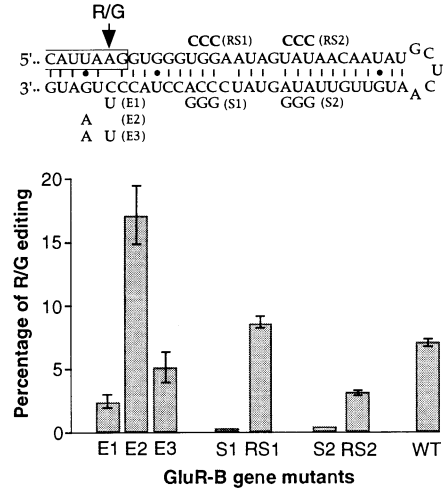

Fig. 2. The dsRNA structure mediating R/G editing of GluR-B transcripts. The RNA comprising distal exon 13–proximal intron 13 sequences is folded into a hairpin structure showing G-U base pairs and mismatches. Exonic nucleotides are boxed, nucleotide substitutions and their designations are indicated, and R/G editing in PC-12 cells is depicted by bar graphs [wild-type (WT), 500-bp Bgl II–Hind III] (Fig. 1).

AMPA receptors in different types of neurons have remarkably different ion conductance and kinetic properties (*1*), in part as a direct consequence of the molecular makeup of the different AMPA receptors. The architecture of this receptor channel permits combinatorial assembly from a pool of four subunits, termed GluR-A to -D or GluR1 to GluR4 (*2*). Each subunit is encoded by a single gene, and hence the relative expression of each gene largely determines the type of AMPA receptor in a given cell (*3*). Additional complexity arises from two alternatively spliced versions for each subunit, termed flip and flop, which differ in the sequence of a small segment that affects pharmacological properties and channel desensitization (*2*, *4*–*6*) and whose relative amounts in the central nervous system change during development (*7*). Furthermore, in GluR-B the residue in a channel position termed the Q/R site, which is critical for the Ca^{2+} permeability of the agonist-activated receptor channel (*8*), is controlled by site-selective RNA editing (*9*). Q/R site editing operates before intron removal on a double-stranded RNA (dsRNA) structure formed by complementary exonic and intronic sequence (*10*).

In addition to the Q/R site, alternative codons for arginine (R; AGA) and glycine (G; GGA) specify residue 764 in rat, mouse, and human GluR-B and the homologous position of rat GluR-D (*4*, *11*). The Arg^{764} codon is the last codon on exon 13 of the gene encoding GluR-B and is spliced alternatively to either the flop module (exon 14) or the flip module (exon 15). A polymerase chain reaction (PCR)–supported survey of the AMPA receptor subunits in adult rat brain demonstrated that flip and flop forms of GluR-B, GluR-C, and GluR-D transcripts exist in both glycine and arginine versions (GluR-C, position 769; GluR-D, position 765), whereas for GluR-A (position 757) only the arginine version was found. Unspliced GluR-B sequences also possessed codon 764 heterogeneity. These findings suggested that except

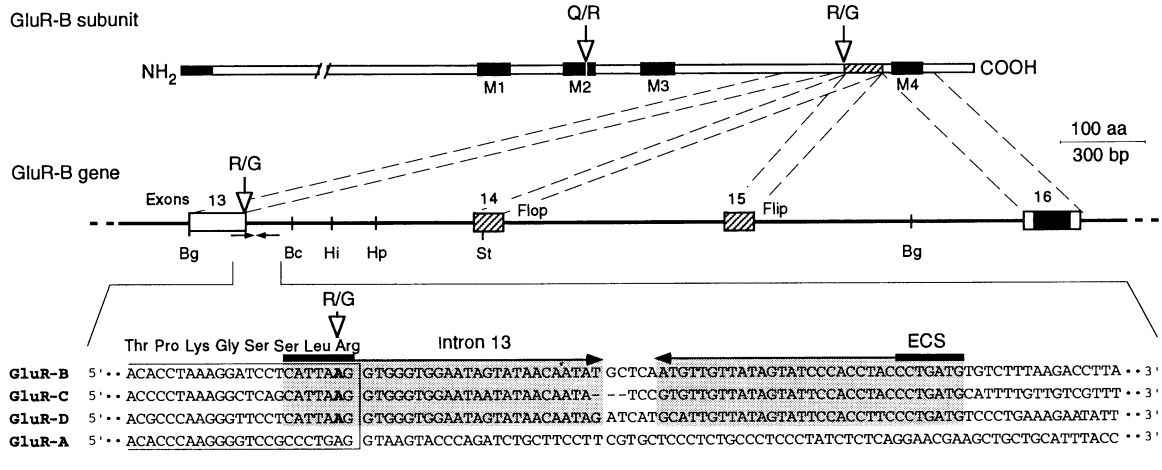

Fig. 1. The R/G site and exon complementary intron sequences in genes encoding AMPA receptors. The GluR-B subunit is depicted with signal sequence and transmembrane regions M1 to M4 (black boxes) and the alternative module flip or flop (shaded box) in front of M4. The Q/R and R/G sites targeted by RNA editing are indicated by open arrowheads. Exons 13 to 16 encoding the GluR-B sequences around the R/G site and intervening introns are drawn to scale (*11*); broken lines connect exons to subunit domains (*4*, *11*). Only restriction sites used for constructing GluR-B minigenes (all start at the Bgl II site in exon 13) are indicated (Bg, Bgl II; Bc, Bcl I; Hi, Hind III; Hp, Hpa I; and St, Stu I). Constructs, approximate sizes, and R/G editing in PC-12 cells were Bgl II–Bcl I, 370 bp, 3.4 ± 0.8% (n = 5); Bgl II–Hind III, 500 bp, 7.0 ± 0.9% (n = 9); Bgl II–Hpa I, 760 bp, 8.5 ± 1.1% (n = 3); Bgl II–Stu I, 1.1 kb, 13.5 ± 1.2% (n = 3); and Bgl II–Bgl II, 2.8 kb, 13.4 ± 1.9% (n = 5). The nucleotide sequences of the distal part of exon 13 and the proximal part of intron 13 are shown for GluR-A to GluR-D. The open arrowhead marks the arginine codon changed by R/G editing, with the targeted adenosine shown in bold. This codon is intersected (vertical line) by the 5′ donor of intron 13. Complementary nucleotide sequences are shaded; horizontal arrows indicate the inverted repeat critical for RNA editing. Complementarity between exonic and intronic sequence (ECS) is indicated by the thickened arrow stems; aa, amino acid.

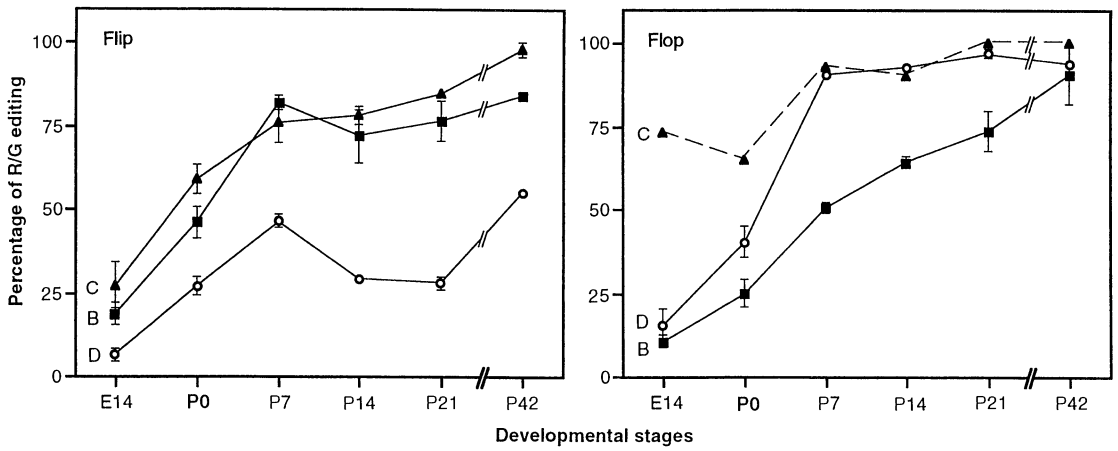

Fig. 3. Developmental progression of R/G editing for the flip and flop splice versions of the GluR-B, -C, and -D subunits. The percentage of R/G site glycine codons in GluR-B to -D subunit cDNAs in their flip (left) and flop (right) versions was determined (*17*) at developmental stages E14 to P42 in rat brains (whole embryos for E14). Data ± SEM are plotted: B, GluR-B (■); C, GluR-C (▲); D, GluR-D (○). The broken line for GluR-C flop indicates that a different method was used (*17*) to evaluate the edited and unedited forms.

for GluR-A, all AMPA receptor subunits may be targeted by nuclear RNA editing to incorporate a glycine residue in the position preceding the flip and flop modules. We termed this position the R/G site.

PC-12 cells from rats and expressing only GluR-B types of AMPA receptor (*12*) were used to determine whether the codon variability in the R/G site is indeed generated by RNA editing. More than 99% of GluR-B transcripts endogenous to PC-12 cells are edited in the Q/R site (*10*) and 26% in the R/G site for both splice forms. Vector constructs harboring exon 13 and intron 13 sequences of the murine AMPA receptor subunit genes (*13*) under the transcriptional control of the human cytomegalovirus promoter-enhancer region (*14*) were transiently expressed in PC-12 cells (*15*). Transcripts derived from these vector constructs were analyzed by reverse transcription–PCR (RT-PCR), followed by probing recombinant phage M13 plaques containing the amplified DNAs with oligonucleotides specific for the alternative R/G site codons (*15*). Large fractional amounts of the R/G site glycine codon were obtained for three of the four genes encoding the subunits (GluR-B, 13.4 ± 1.9%, $n = 5$; GluR-C, 5.5 ± 1.0%, $n = 3$; and GluR-D, 17.4 ± 3.0%, $n = 3$), indicating that RNA editing generates codon variability in these gene transcripts. Analogous to Q/R site editing (*10*), R/G site editing levels of exogenous sequences were lower than those for the endogenously expressed GluR-B sequence (*10*). The failure of PC-12 cells to edit the GluR-A gene sequence (no G form, $n = 2$) is consistent with the lack of in vivo editing for this gene and might reflect the absence of an intronic element, analogous to the editing site complementary sequence (ECS) for Q/R site editing (*10*). Indeed, DNA sequence analysis located such an element in the proximal part of intron 13 in the genes encoding GluR-B, -C, and -D but not in GluR-A (Fig. 1).

Table 1. Functional differences of AMPA receptor channels edited and unedited at the R/G site. Flip, i; flop, o; R, arginine; G, glycine. The t_{rec} values describe the decay phase of the time-dependent depression of the current response to the second agonist pulse. The percentages of maximal depression of the current response to the second agonist pulse are from the same set of experiments. The peak to steady-state current ratios were calculated from desensitization experiments (current amplitude at the peak and average current amplitude 50 to 59 ms after agonist application). All values are mean ± SD, except for the ratio of the peak current to the steady state current (I_{peak}/I_{ss}), which is mean ± SEM. t_{des}, desensitization time constant. Numbers in parentheses are the number of patches recorded.

GluR type	t_{rec} after 1-ms prepulse (ms)	Maximal depression of second pulse (%)	t_{des} (60-ms application) (ms)	I_{peak}/I_{ss}
$C_i(R)$	36 ± 7 (3)	35 ± 7	4.0 ± 0.5 (12)	41 ± 6 (12)
$C_i(G)$	15 ± 6 (4)	24 ± 4	4.9 ± 0.6 (8)	36 ± 9 (8)
$D_i(R)$	14 ± 4 (8)	24 ± 5	3.6 ± 0.6 (10)	180 ± 50 (9)
$D_i(G)$	6 ± 2 (15)	11 ± 3	6.6 ± 1.0 (21)	25 ± 4 (21)
$D_o(R)$	43 ± 9 (5)	79 ± 7	1.6 ± 0.2 (8)	390 ± 70 (8)
$D_o(G)$	31 ± 3 (12)	93 ± 5	0.9 ± 0.1 (19)	310 ± 50 (16)
$A_i(R)/B_o(R)$	67 ± 17 (7)	62 ± 11	3.5 ± 0.5 (12)	130 ± 30 (7)
$A_i(R)/B_o(G)$	37 ± 8 (7)	57 ± 4	3.5 ± 0.7 (13)	140 ± 15 (13)
$A_i(R)/B_i(R)$	61 ± 15 (5)	59 ± 10	3.2 ± 0.6 (9)	230 ± 50 (9)
$A_i(R)/B_i(G)$	28 ± 4 (10)	31 ± 5	5.4 ± 1.0 (28)	120 ± 40 (22)
$B_i(G)/C_i(R)$	26 ± 4 (9)	33 ± 3	4.2 ± 0.7 (9)	67 ± 15 (14)
$B_i(G)/C_i(G)$	15 ± 3 (8)	28 ± 4	4.9 ± 0.8 (19)	46 ± 8 (19)

The presence of the ECS site predicted (*10*) that the putative exon-intron dsRNA (Fig. 2) is involved in R/G editing. We tested this by introducing nucleotide substitutions (*16*) in a murine GluR-B gene construct [500-bp Bgl II–Hind III fragment (Fig. 1)], which yielded 7.0 ± 0.9% ($n = 9$) R/G editing in PC-12 cells (Fig. 2). When two blocks of three consecutive intronic nucleotides in the predicted stem region of the dsRNA were replaced by guanosines to generate mutants S1 and S2 (Fig. 2), R/G editing dropped to nearly undetectable levels (<0.2%; $n = 4$). Editing of these mutants was partly restored by substituting cytosines for correct base paring in the complementary exonic sequence [double mutants RS1 (8.5 ± 0.5%; $n = 3$) and RS2 (3.1 ± 0.2%; $n = 4$)]. Mutations in the intronic ECS sequence had variable effects. The mutant E1, which contains a point mutation opposite of the adenosine that is to be edited, decreased the extent of R/G editing (2.2 ± 0.5%; $n = 4$). The point mutation E2, designed to stabilize the stem of the exon-intron dsRNA, increased the percentage of editing by more than twofold (17 ± 2%; $n = 5$), and the double mutant E3 yielded 5 ± 1% ($n = 3$) R/G editing. Overall, these data indicate that the sequence-predicted dsRNA structure is essential for R/G editing, as observed for Q/R site editing (*10*). Furthermore, GluR-B gene

H. Lomeli, T. Melcher, T. Kuner, H. Monyer, M. Higuchi, P. H. Seeburg, Laboratory of Molecular Neuroendocrinology, Center for Molecular Biology (ZMBH), University of Heidelberg, 69120 Heidelberg, Germany.
J. Mosbacher and J. R. P. Geiger, Max-Planck-Institut für Medizinische Forschung, 69120 Heidelberg, Germany.
T. Höger and A. Bach, BASF AG, 67056 Ludwigshafen, Germany.

*Present address: Instituto de Biotecnologia, Universidad Nacional Autonoma de Mexico, APDO.510-3, Cuernavaca Morelos 62271, Mexico.
†To whom correspondence should be addressed.

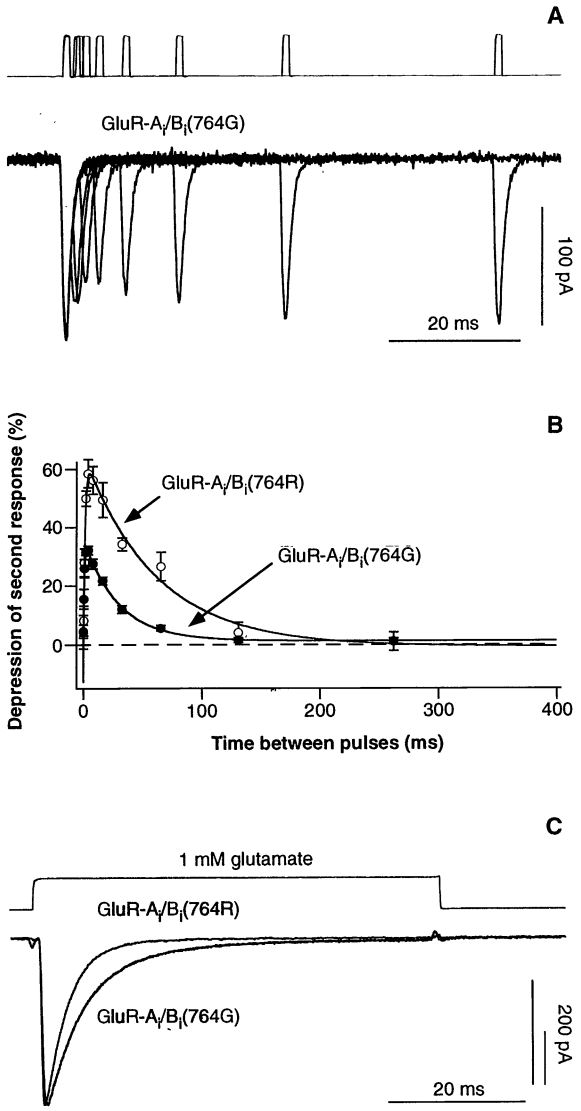

Fig. 4. Differences in the time courses of desensitization and recovery from desensitization for heteromeric GluR-A/B AMPA receptors. Flip, i; flop, o; R, arginine; G, glycine. (**A**) Several superimposed current traces mediated by GluR-A$_i$/B$_i$(764G) channels were obtained by a 1-ms double-pulse protocol. The time interval between two pulses was 0.5 ms for the first pulse and was increased by a factor of 2 for the following pulses. The holding potential was −40 mV. The upper trace is the open tip response to an application of normal frog Ringer solution (diluted 10 times) (*6*) with the same pulse sequence, reflecting the time of glutamate application. (**B**) The depression of the peak current amplitudes in response to the second glutamate pulse in relation to the first current response is shown versus the time interval between the two pulses. The lines represent the double-exponential functions (as a superposition of the exponential rising phase and the exponential decay phase) fitted to pooled data (n = 11 and 5), with decay time constants of 28 and 61 ms for the GluR-A$_i$/B$_i$(764G) (●) and GluR-A$_i$/B$_i$(764R) (○) channels, respectively. The onsets of desensitization as estimated by the rising phase of the depression had time constants of 0.5 and 1.3 ms; the maximal percentages of desensitized channels by the 1-ms prepulse were 31 and 59%, respectively. Error bars are SEM. (**C**) Current traces mediated by GluR-A$_i$/B$_i$(764G) and GluR-A$_i$/B$_i$(764R) channels to an application of 1 mM glutamate for 60 ms were superimposed and scaled to their peak amplitude. The holding potential was −40 mV, and each trace represents an average of 10 single pulse responses. The small peaks at the beginning and at the end of the glutamate pulse are caused by the high voltage driving the piezo element for the fast application system. The upper trace shows the open tip response after disruption of the patch.

constructs containing the ECS site and progressive lengths of intron 13 and beyond yielded increasing extents of R/G site editing, from 3 to 14% (Fig. 1). The point mutation E2 more than doubled R/G editing in all constructs (the E2 mutation was introduced into the Bgl II–Bgl II construct; 35.0 ± 2.5%; n = 4), and the longest construct (Bgl II–Bgl II) (Fig. 1) when carrying the intronic block mutation S1 (Fig. 2) was virtually unedited (<0.2%, n = 2). Thus, unlike Q/R site editing distal intron sequences, although not prerequisite for R/G site editing, increase editing efficiency.

We studied the extent of editing at the R/G site in the alternatively spliced flip and flop versions of the GluR-B, -C, and -D subunits during rodent brain development (*17*). The extent of R/G editing in the embryonal brain is generally small for both splice forms but increases dramatically during development (Fig. 3). Differences are apparent in the extent of R/G editing for the alternative splice forms of a subunit, perhaps indicating that different cell types edit the R/G site to different extents. This is exemplified for GluR-D, whose flip version manifests a biphasic developmental progression and, in the adult rat brain, has 55% R/G editing. The most likely explanation is that cerebellar Bergmann glial cells, which proliferate postnatally and express large amounts of GluR-D flip (*7*), do not edit the R/G site. This was corroborated by single-cell PCR analysis (*3*, *18*, *19*) of eight Bergmann glial cells harvested by a patch pipette in postnatal day 15 (P15) rat cerebellar slices (*20*). Besides GluR-A, these cells contained only the R form of GluR-D flip, consistent with our observation that in adult rat cerebellum only about 10% of GluR-D flip has R/G editing. In contrast, 95% of cerebellar GluR-D flop sequences are edited, and this form is prominently expressed in late postnatal stages by the abundant cerebellar granule cell population (*7*).

We investigated the functional differences between the R and G forms of AMPA receptors by expressing the appropriate complementary RNAs in *Xenopus* oocytes (*21*). We determined values for the median effective concentration (EC_{50}) for the glutamate-activated steady-state currents, because the region around the R/G site and the flip-flop modules may be a part of an extracellularly located bipartite agonist binding site (*2*, *22*). The EC_{50} values increased for edited forms, but this effect was not observed for all channels (*21*). We then analyzed recombinant channels in outside-out patches excised from oocytes, using a fast application system for L-glutamate (*23*). For all channels tested, the 20 to 80% rise time of current was on average less than 0.5 ms, and the time constant of deactivation after rapid removal of glutamate was on average less than 1 ms. These values did not appear to differ for channel forms with or without R/G site editing.

We next measured the recovery of macroscopic current responses from desensitization by applying two 1-ms pulses of 1 mM glutamate separated by increasing time intervals. This short-pulse protocol may mimic the synaptic situation where the glutamate concentration peaks around 1 mM for about 1 ms (*24*). The time course of recovery from desensitization was affected by the subunit configuration and, for a given configuration, consistently by the R/G site (Table 1). All recovery time courses could be fitted well by monoexponential functions described by the time constant t_{rec}. GluR-A$_i$/B$_i$(764G) channels, a subunit combination likely to occur in neurons (*3*, *4*, *7*), are characterized by a t_{rec} value of 28 ms (Fig. 4A), whereas GluR-A$_i$/B$_i$(764R) channels show a t_{rec} of 61 ms (Table 1), indicating considerably faster recovery from desensitization when GluR-B$_i$ has R/G editing. Plotting the depression of the current response to the second agonist pulse as a function of the duration of the interpulse interval (Fig. 4B) illustrates that only half as many GluR-A$_i$/B$_i$(764G) channels (31%) as GluR-A$_i$/B$_i$(764R) channels (59%) are maximally desensitized after a 1-ms prepulse of 1 mM glutamate. Hence, for a given subunit configuration, channels with R/G editing respond to agonist even after a very short time interval after the prepulse (Table 1). The t_{rec} values (6 to 70 ms) cover the same approximate range recorded in channels from central neurons (9 to >100 ms) (*25*, *26*). Because of faster recovery and a ten-

dency for slower desensitization rates, the edited versions of AMPA receptors show larger steady-state currents than the unedited forms (Fig. 4C and Table 1).

Thus, in addition to cellular control over the expression of the individual subunit genes (*3*), the size and shape of the fast component of excitatory postsynaptic currents (EPSCs) can be determined by the developmentally directed interplay of alternative splicing and R/G editing. Desensitization may shape the decay phase of a single EPSC (*25*) but is in many cells slower than the decay of EPSCs (*25*, *26*). The rate of desensitization determines the fraction of channels that are desensitized by a glutamate pulse and hence, together with the recovery rate, controls the excitability of a single postsynaptic site in response to subsequent stimuli. Fast desensitizing, slowly recovering AMPA receptors should respond only to the beginning of a sequence of fast stimuli, whereas rapidly recovering receptors should integrate the incoming signals as they will transmit virtually undepressed an entire train of fast stimuli.

REFERENCES AND NOTES

1. P. Jonas and N. Spruston, *Curr. Opin. Neurobiol.* **4**, 366 (1994); L. O. Trussell, I. M. Raman, S. Zhang, *Semin. Neurosci.* **6**, 71 (1994).
2. P. H. Seeburg, *Trends Neurosci.* **16**, 359 (1993).
3. P. Jonas, C. Racca, B. Sakmann, P. H. Seeburg, H. Monyer, *Neuron* **12**, 1281 (1994).
4. B. Sommer *et al.*, *Science* **249**, 1580 (1990).
5. K. M. Partin, D. K. Patneau, M. L. Mayer, *Mol. Pharmacol.* **46**, 129 (1994).
6. J. Mosbacher *et al.*, *Science*, in press.
7. H. Monyer, P. H. Seeburg, W. Wisden, *Neuron* **6**, 799 (1991).
8. M. Hollmann, M. Hartley, S. F. Heinemann, *Science* **252**, 851 (1991); R. I. Hume, R. Dingledine, S. F. Heinemann, *ibid.* **253**, 1028 (1991); N. Burnashev, H. Monyer, P. H. Seeburg, B. Sakmann, *Neuron* **8**, 189 (1992).
9. B. Sommer, M. Köhler, R. Sprengel, P. H. Seeburg, *Cell* **67**, 11 (1991); M. Köhler, N. Burnashev, B. Sakmann, P. H. Seeburg, *Neuron* **10**, 491 (1993).
10. M. Higuchi, *et al.*, *Cell* **75**, 1361 (1993).
11. M. Köhler, H. C. Kornau, P. H. Seeburg, *J. Biol. Chem.* **269**, 17367 (1994).
12. M. Higuchi, T. Höger, P. H. Seeburg, unpublished results.
13. A murine 3.4-kb Sal I–Eco RI GluR-B gene fragment spanning intron 12 to exon 16 (*11*) and cloned into pBluescript (Stratagene) was the source for the DNA sequence of GluR-B intron 13 and for minigenes constructed in the eukaryotic expression vector pRK (*14*). All GluR-B minigenes [Bgl II–Bcl I (370 bp); Bgl II–Hind III (500 bp); Bgl II–Hpa I (760 bp); Bgl II–Stu I (1.1 kb); and Bgl II–Bgl II (2.8 kb)] started with the Bgl II site at the beginning of exon 13 (Fig. 1). The GluR-C intron 13 sequence was from a murine genomic clone. A 520-bp DNA fragment (exon 13 plus 320 bp of intron 13) was PCR-amplified with primers Cex13 (5′-CGCAATTCCGCAGAGCCATCTGTGTTTA-3′) and intC1 (5′-GCAAGCTTCAAGAACACCACATCCATGC-3′). For GluR-D, a 1-kb Xba I–Eco RI fragment containing the entire exon 13 and approximately 750 bp of intron 13 was isolated from a 4-kb Sal I–Eco RI murine genomic clone in pBluescript. For GluR-A, a 920-bp DNA fragment containing the entire exon 13 and 670 bp of intron 13 was PCR-amplified from a genomic clone with primers Aex13 (5′-CCGAATTCTCTAAAATCGCTGTGTTTGAG-3′) and Aint13-670 (5′-GTAGCAAATTCTAGAATTAACTC-3′).
14. T. J. Schall *et al.*, *Cell* **61**, 361 (1990).
15. PC-12 cells (American Type Culture Collection CRL 1721) were transfected and processed as described (*10*). Construct-derived sequences were PCR-amplified [K. B. Mullis and F. A. Faloona, *Methods Enzymol.* **155**, 335 (1987)] with rsp23 (5′-CGGATTCCCCGTGCCAAGAGTGAC-3′) as 5′ primer (*10*) and 3′ primers specific for the individual intron 13 sequences [intA13-200, 5′-GCGGTACCCGTCAAAAGCAAGCTGAGGC-3′; intB1, 5′-GCGGTACCGTGAGTTACCTCATATCCGTAT-3′; intC1 (*13*); and intD1, 5′-GCGGTACCGCTTTTACCTGATTGTTGATC-3′]. For the short GluR-B Bgl II–Bcl I construct, cis33 (*10*) was used as 3′ primer. PCR products were directionally cloned into phage M13mp18 RF-DNA [C. Yanisch-Perron, J. Vieira, J. Messing, *Gene* **33**, 103 (1985)]. One set of dual filter lifts from phage plates was probed for recombinant plaques; the other filter set was hybridized with 20-mer oligonucleotides complementary to the exon-intron 13 boundary of the genes encoding GluR-A to GluR-D to distinguish R forms from G forms (*17*).
16. Nucleotide substitutions were introduced by PCR-mediated mutagenesis [R. M. Horton, H. D. Hunt, S. N. Ho, J. K. Pullen, L. R. Pease, *Gene* **77**, 61 (1990)] into the Bgl II–Hind III GluR-B minigene (Fig. 1) cloned in the expression vector pRK (*14*). Each nucleotide substitution was contained in a pair of complementary 20-base PCR primers. Mutants and mutagenesis primers (only sense strand is given) were E1, 5′-CCACCTACCTTGATGTGTCT-3′; E2, 5′-CCACCTACCCTAATGTGTCT-3′; E3, 5′-CCACCTACCTTAATGTGTCT-3′; S1, 5′-TATAGTATCGGGCCTACCCT-3′; S2, 5′-AATGTTGTTGGGGTATCCCA-3′; RS1, 5′-TAAGGTGGGCCCAATAGTAT-3′; and RS2, 5′-GTGGAATAGCCCAACAATAT-3′. The sense primer was used as a 5′ primer; the cis33 oligonucleotide (*10*) served as the 3′ primer. The antisense mutant primer was used in combination with the vector-specific 5′ primer rsp23 (*10*). Partner PCR fragments were gel-isolated, combined, and denatured, and the mutated DNA fragment was amplified with PCR primers rsp23 and cis33. Amplified DNAs were digested with Eco RI and Hind III and cloned into pRK (*14*).
17. Total RNA isolated from embryonic day 14 (E14) embryos and from the brains of P0, P7, P14, P21, and P42 rats was reverse-transcribed with random hexamers. For each stage, three animals were analyzed individually. The complementary DNAs (cDNAs) served as templates for PCR amplifications (35 cycles; 30 s, 94°C; 30 s, 55°C; and 40 s, 72°C) of the four subunit sequences. Subunit-specific 5′ primers were A51, 5′-GCGAATTCGAGGGACGAGACCAGACAACC-3′; B52, 5′-GCGAATTCACACAAAGTAGTGAATCAACT-3′; C52, 5′-CCGAATTCACAAAGCCCTCCTGATCCTC-3′; and D51, 5′-GCGAATTCCTGAGGATGGGAAGGAAGG-3′; the common 3′ primer was 3′lamlo, 5′-GCGGTACCTCGTACCACCATTTG(TC)TTTTCA-3′ (*19*). The GluR-A sequence was amplified from P42 brains only. Primers B52 and 3′lamlo were also used to amplify endogenous GluR-B transcripts in PC-12 cells. All PCR products (~630 bp) were directionally cloned into M13mp18 RF-DNA cleaved with Eco RI and Kpn I. Dual filter lifts of recombinant phage plates (>400 plaques each) were probed with oligonucleotides (21-mers) having exact complementarity to the flip and flop forms with R/G editing. The R/G codon variability in the cloned sequences was revealed by the stringency of filter washing, established separately for each subunit sequence. Typically, filters were hybridized in 10% formamide and 5× saline sodium citrate (SSC) at ambient temperature and were washed at 45°C in 0.5× SSC. Under these conditions, plaques carrying the unedited R/G sequence had a lower signal intensity than the edited sequence, which was confirmed by DNA sequencing. We could not design oligonucleotide probes to distinguish the GluR-C flop forms with or without R/G editing. These were evaluated by sequencing for each animal and developmental stage 25 recombinant M13 DNAs containing the GluR-C flop sequence.
18. R. N. van Gelder *et al.*, *Proc. Natl. Acad. Sci. U.S.A.* **87**, 1663 (1990); P. Bochet *et al.*, *Neuron* **12**, 383 (1994).
19. B. Lambolez, E. Audinat, P. Bochet, F. Crépel, J. Rossier, *Neuron* **9**, 247 (1992).
20. Parasagittal 300-μm-thick cerebellar slices from 15-day-old Wistar rats were continuously superfused with physiological extracellular solutions. Cells were visualized with infrared-differential interference contrast video microscopy [H. U. Dodt and W. Zieglgänsberger, *Brain Res.* **537**, 333 (1990)] as described (*3*). Bergmann glia cells, identified by their radial processes and close apposition to Purkinje cells, were analyzed as described [G. J. Stuart, H. U. Dodt, B. Sakmann, *Pflueger Arch.* **423**, 511 (1993)]. Resistances of patch pipettes were between 1 and 3 megohms, and the pipettes were filled with 8 μl of 140 mM KCl, 5 mM EGTA, 3 mM $MgCl_2$, and 5 mM Hepes (pH 7.3; KOH). Typical for glial cells, the patch pipette formed a spontaneous seal, the input resistance was low (20 to 30 megohms), cells had a resting potential of −80 mV, and depolarization steps documented the absence of Na^+ currents. The cytoplasms and nuclei of Bergmann glial cells were harvested into the patch pipette, and the pipette contents were analyzed by RT-PCR for AMPA receptor subunit–specific sequences as described (*3*), except that the second PCR reaction was primed in separate tubes with the use of nested subunit-specific primers [A51, B52, C52, and D51 (*17*)]. For all Bergmann glial cells harvested, DNA products were obtained only for GluR-A and GluR-D, and these were cloned in M13mp18 RF-DNA for the evaluation of alternative splice forms and R/G variability (*17*).
21. An arginine codon was substituted for the glycine codon in the R/G site of flip and flop versions of cloned GluR-B and GluR-C cDNAs and in GluR-D flop cDNA (*4*). In cloned GluR-D flip cDNA (*4*), the arginine codon was exchanged for a glycine codon. Mutagenesis was performed on the single-stranded form of the recombinant pRK vectors with the use of 24-base oligonucleotides. Suitable DNA fragments were then exchanged between the codon-substituted recombinant pRK vectors and oocyte expression vectors carrying the cloned AMPA receptor cDNAs. The latter vectors, derived from pSP64T [D. A. Melton *et al.*, *Nucleic Acids Res.* **12**, 7035 (1984)], were linearized immediately 3′ of the polyadenylate sequence, and cRNAs were synthesized in vitro with SP6 polymerase. *Xenopus* oocytes were injected with 10 to 20 ng of cRNA and incubated for 3 to 6 days at 19°C. We obtained heteromeric channels by injecting equal amounts of the respective cRNAs. EC_{50} values of glutamate for steady-state currents were obtained in whole-cell configuration at −70 mV as described [E. Stein, J. A. Cox, P. H. Seeburg, T. A. Verdoorn, *Mol. Pharmacol.* **42**, 864 (1992)]. For example, for GluR-A/B channels these values were GluR-A_i/B_i(764G), 22.6 ± 3.2 μM, n = 8; GluR-A_i/B_i(764R), 10.5 ± 0.5 μM, n = 2; GluR-A_o/B_i(764G), 17.5 ± 2.5 μM, n = 6; and GluR-A_o/B_i(764R), 16.4 ± 2.2 μM, n = 4. Dose-response curves for peak currents could not be measured because outside-out patches had currents that decayed over time and an average stability of only 5 min. Patch recordings with a fast application system were performed as described (*6*). For double-pulse experiments, we analyzed the recovery from desensitization by plotting 100% $[1 - I(t_0 + \Delta t)/I(t_0)]$ versus Δt, where $I(t_0)$ and $I(t_0 + \Delta t)$ are the current peak amplitudes of the first and second pulse, respectively, and Δt is the time interval between the two pulses. A double-exponential function was fitted to the pooled data points, with one exponential describing the rising and the other one the decaying phase of depression of the second peak amplitude. We obtained desensitization time constants by fitting a monoexponential function to the decay phase of current evoked by a 60-ms pulse of 1 mM glutamate.
22. N. Nakanishi, N. A. Shneider, R. Axel, *Neuron* **5**, 569 (1990); K. W. Roche, L. A. Raymond, C. Blackstone, R. L. Huganir, *J. Biol. Chem.* **269**, 11679 (1994); F. A. Taverna, L. Y. Wang, J. F. MacDonald, D. R. Hampson, *ibid.*, p. 14159.
23. C. Franke, H. Hatt, J. Dudel, *Neurosci. Lett.* **77**, 199 (1987).
24. J. P. Clements, R. A. J. Lester, G. Tong, C. E. Jahr, G. L. Westbrook, *Science* **258**, 1498 (1992).
25. L. O. Trussell and G. D. Fischbach, *Neuron* **3**, 209

(1989); S. Hestrin, *ibid.* **9**, 991 (1992); L. O. Trussell, S. Zhang, I. M. Raman, *ibid.* **10**, 1185 (1993); B. Barbour, K. U. Keller, I. Llano, A. Marty, *ibid.* **12**, 1331 (1994).
26. D. Colquhoun, P. Jonas, B. Sakmann, *J. Physiol. (London)* **458**, 261 (1992); P. Jonas and B. Sakmann, *ibid.* **455**, 143 (1992).
27. B. Sommer provided the cloned and sequenced murine GluR-C gene segment. We thank S. Grünewald for cell culture, A. Herold for DNA sequencing, and J. Rami for assistance with the manuscript. We gratefully acknowledge the input and support of R. Sprengel, A. Ultsch, P. Jonas, and B. Sakmann. T.M. and J.R.P.G. were supported by the graduate program of Molecular and Cellular Neurobiology of Heidelberg University. Funded by Sonderforschungsbereich 317 grants B/9 and B/14 and Deutsche Forschungsgemeinschaft grant Mo 432/2-1.

29 July 1994; accepted 28 September 1994

Resetting the Biological Clock: Mediation of Nocturnal Circadian Shifts by Glutamate and NO

Jian M. Ding, Dong Chen, E. Todd Weber, Lia E. Faiman, Michael A. Rea, Martha U. Gillette*

Circadian rhythms of mammals are timed by an endogenous clock with a period of about 24 hours located in the suprachiasmatic nucleus (SCN) of the hypothalamus. Light synchronizes this clock to the external environment by daily adjustments in the phase of the circadian oscillation. The mechanism has been thought to involve the release of excitatory amino acids from retinal afferents to the SCN. Brief treatment of rat SCN in vitro with glutamate (Glu), *N*-methyl-D-aspartate (NMDA), or nitric oxide (NO) generators produced lightlike phase shifts of circadian rhythms. The SCN exhibited calcium-dependent nitric oxide synthase (NOS) activity. Antagonists of NMDA or NOS pathways blocked Glu effects in vitro, and intracerebroventricular injection of a NOS inhibitor in vivo blocked the light-induced resetting of behavioral rhythms. Together, these data indicate that Glu release, NMDA receptor activation, NOS stimulation, and NO production link light activation of the retina to cellular changes within the SCN mediating the phase resetting of the biological clock.

Diurnal oscillations of endocrine, physiological, and behavioral functions are ubiquitous features of eukaryotes (*1*). In mammals, the mechanisms responsible for the generation and synchronization of these circadian rhythms reside in the hypothalamic SCN (*2*). The dominant signal that coordinates internal time with environmental changes is light. Photic information is conveyed to the SCN by way of a direct retinal projection, the retinohypothalamic tract (*3*). Under conditions of continuous darkness, brief light exposure during the early subjective night causes phase delays, whereas exposure during the late subjective night causes phase advances of circadian rhythms driven by the SCN clock (*4*). Light exposure during the subjective day does not alter the circadian phase. Neither the mechanisms responsible for clock resetting, nor those underlying nocturnal restriction, or "gating," of the response are understood.

Glutamate (Glu) is the putative neurotransmitter that mediates photic entrainment. Glu and its bipeptide precursor are localized in retinal fibers innervating the SCN, and Glu is released after optic nerve stimulation in vitro (*5*). Antagonists of the NMDA subtype of Glu receptor block photic phase shifts of the free-running activity rhythm in rodents (*6*, *7*). Although attempts to affect phase in vivo by Glu with bolus injections near the SCN have failed to elicit lightlike effects on circadian rhythms (*8*), preliminary reports suggest that SCNs in vitro show nocturnal sensitivity to Glu (*9*).

Activation of NMDA Glu receptors in neural systems leads to an influx of Ca^{2+}. This, in turn, can activate nitric oxide synthase (NOS), resulting in the production of nitric oxide (NO) (*10*). NO is a short-lived gaseous neurotransmitter that can readily traverse cell membranes and produce intercellular effects. Thus, NO can activate guanylate cyclase or adenosine diphosphate–ribosyltransferase or facilitate neurotransmitter release in cells neighboring the site of NOS stimulation (*11*).

In order to selectively probe the pathway of phase resetting of the biological clock, we studied a SCN rat brain slice preparation maintained in vitro for 3 days (*12*). The mean firing frequency of SCN neurons in vitro forms a sinusoidal curve, with a 24-hour period and a peak midday, near circadian time 7 (CT 7) (Fig. 1A) (*13*). A microdrop of 10 mM Glu was briefly applied to the SCN and the time of subsequent peaks in neuronal activity assessed (*14*). Glu induced robust phase shifts, depending on the phase of the circadian cycle at which it was administered (Fig. 1, B through D). When applied to the SCN in the early subjective night, Glu caused a 3.0-hour delay in the neuronal circadian rhythm. Peak activity remained delayed by the same interval relative to the normal peak for the 2 days studied after Glu treatment, indicating that a stable phase resetting of the SCN clock had been induced. Later in the subjective night, Glu application advanced

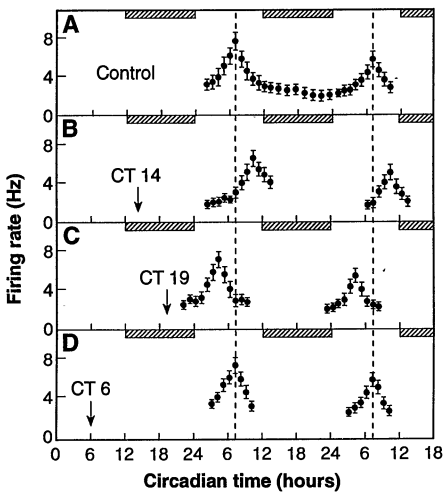

Fig. 1. Sensitivity of the SCN to phase resetting by Glu. We assessed sensitivity by measuring the phasing of endogenous circadian rhythms of neuronal firing rate of the SCN in brain slices (*14*). Circadian rhythms of the ensemble of neurons were derived by random sampling of single units extracellularly at 10-min intervals for two 2-min periods. Units (82 to 124) were sampled per slice; activities were grouped into a 2-hour running average ± SEM to determine the time of peak firing activity (*13*). (**A**) Circadian rhythms of neuronal activity in SCN slices in vitro shown in a continuous record over 38 hours from a single SCN on days 2 to 3 after slice preparation. The horizontal bars indicate the subjective night of the circadian cycle. The dashed vertical lines mark the time of the normal peak activity at CT 7 in unperturbed and EBSS-treated controls (*13*). (**B**) Effect of Glu at CT 14 on the activity rhythm. A 0.2-μl droplet of 10 mM Glu was applied directly to the SCN for 10 min (arrow), followed by EBSS rinse, during the early subjective night at CT 14. (**C**) Effect of Glu at CT 19. (**D**) Effect of Glu at mid-subjective day, CT 6.

J. M. Ding, Department of Cell and Structural Biology and the Neuroscience Program, University of Illinois, 506 Morrill Hall, 505 South Goodwin Avenue, Urbana, IL 61801, USA.
D. Chen and E. T. Weber, Department of Physiology, University of Illinois, 524 Burrill Hall, 407 South Goodwin Avenue, Urbana, IL 61801, USA.
L. E. Faiman, Department of Cell and Structural Biology, University of Illinois, 506 Morrill Hall, 505 South Goodwin Avenue, Urbana, IL 61801, USA.
M. A. Rea, Biological Rhythms and Integrative Neuroscience Research Institute, Armstrong Laboratory (CFTO), 2504 Gillingham Drive, Suite 1, Brooks Air Force Base, TX 78235–5104, USA.
M. U. Gillette, Departments of Cell and Structural Biology and Physiology and the Neuroscience Program, University of Illinois, 506 Morrill Hall, 505 South Goodwin Avenue, Urbana, IL 61801, USA.
*To whom correspondence should be addressed.